

# A Comparative Study of Co-Channel Interference Suppression Techniques\*

Jon Hamkins

hamkins@jpl.nasa.gov

818-354-4764

Jet Propulsion Laboratory

48000ak Grove Dr.

Pasadena, CA 91 109-8099

Ed Satorius

satorius@bvd.jpl.nasa.gov

818-354-5790

Gent Paparisto

paparist@milly.usc.edu

213-740-4673

Electrical Engineering — Systems

University of Southern California

Los Angeles, CA 90089-2565

Andreas Polydoros

andreas@solar.usc.edu

213-740-4667

## ABSTRACT

We describe three methods of combating co-channel interference (CCI): across-coupled phase-locked loop (CCPLL); a phase-tracking circuit (PTC), and joint Viterbi estimation based on the maximum likelihood principle. In the case of co-channel FM-modulated voice signals, the CCPLL and PTC methods typically outperform the maximum likelihood estimators when the modulation parameters are dissimilar. However, as the modulation parameters become identical, joint Viterbi estimation provides for a more robust estimate of the co-channel signals and does not suffer as much from "signal switching" which especially plagues the CCPLL approach. Good performance for the PTC requires both dissimilar modulation parameters and a priori knowledge of the co-channel signal amplitudes. The CCPLL and joint Viterbi estimators, on the other hand, incorporate accurate amplitude estimates. In addition, application of the joint Viterbi algorithm to demodulating co-channel digital (BPSK) signals in a multipath environment is also discussed. It is shown in this case that if the interference is sufficiently small, a single trellis model is most effective in demodulating the co-channel signals.

## INTRODUCTION

Co-channel interference (CCI) can be a serious impairment to any communication system. In this paper, we first focus on separating two CCIFM signals of the form

$$r(t) = A_1 \cos(\omega_1 t + \theta_1(t)) + A_2 \cos(\omega_2 t + \theta_2(t)), \quad (1)$$

where  $E_i(t) = k_i \int_{-\infty}^t m_i(s) ds$  and  $m_i(t)$  are the modulating signals. (Subsequently, we will consider the demodu-

lation of co-channel digitally modulated (BPSK) signals in the presence of multipath.) As evident from the model described by Equation (1), each FM signal alone has a constant envelope and an instantaneous frequency which is proportional to its modulating signal; on the other hand,  $r(t)$  has a widely varying envelope and an instantaneous frequency which contains large spikes. A conventional FM receiver containing a single PLL may be able to correct for the varying envelope with the use of a hard limiter, but the spikes will remain and  $m_1(t)$ ,  $m_2(t)$ , and  $m_1(t) + m_2(t)$  are each unrecoverable. Ideally,  $m_1(t)$  and  $m_2(t)$  are recovered separately, with no crosstalk between the two.

There are several approaches to CCI suppression which are based on either linear or non-linear processing. Linear processing methods encompass narrowband linear filtering as well as adaptive filtering techniques which suppress interference based on statistical differences between the interference and desired signal components. Examples of adaptive interference suppression filtering techniques include linear prediction error filtering as well as "blind" adaptive processing wherein linear filter coefficients are adjusted to enhance certain properties of the desired signal (thereby suppressing the interference).

Non-linear techniques are usually based upon the "capture" effect wherein the strongest signal is enhanced by some type of non-linearity at the expense of weaker signals which are suppressed. Since these techniques are dependent on the relative amplitudes of the various signal components, they can be utilized for separating multiple components with highly overlapped spectra. Examples include the FM limiter/discriminator, PLL, PTC [3], CCPLL [2,6], and maximum likelihood (ML) -based techniques [1,5].

## CCPLL AND PTC METHODS

The CCPLL and PTC techniques fall within a class of

\*The research described in this paper was carried out by the Jet Propulsion Laboratory, California Institute of Technology, under a contract with the National Aeronautics and Space Administration.

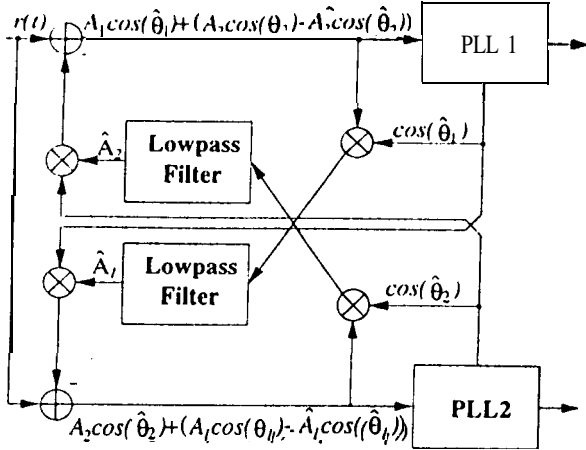


Figure 1: CCPLL block diagram.

methods that exploit the capture property of the PLL to separate co-channel signals. The **CCPLL** comprises two PLLs: one used to capture the dominant signal and the second to capture the sub-dominant (its architecture can easily be extended to separate multiple signals). A simplified block diagram, based on the feed-forward, **difference-amplitude tracking** topology developed in [7], is illustrated in Figure 1. We note that both PLLs are **second-order**, incorporating proportional plus integral control, and both **lowpass** filters, used in generating the amplitude estimates, are second-order digital Butterworth designs.

Although this method has been proposed for separating a wide variety of signals including CW, FM, AM and even digital signals, e.g., BFSK, we have found that for **cases** of co-channel signals with comparable modulation parameters the CCPLL becomes less effective. As an illustrative example, consider the case of two synthesized voice signals (approximately 3.7 kHz bandwidth) that are FM-modulated. The parameters from Equation (1) are  $A_1 = 1$ ,  $A_2 = 0.5$ ,  $k_1 = k_2 = 2\pi(12\text{kHz})$ , and  $\omega_1 = \omega_2 = 0$  (i.e., baseband). Thus the weaker (sub-dominant) signal is 6 dB below the dominant. The signal was sampled at 131kHz. Using the CCPLL design rules developed in [6], we obtain sample computer simulation results as depicted in Figure 2 for a three second segment. Both the original and CC PLL-reconstructed estimates (demodulated by the PLLs) for the dominant and sub-dominant synthesized voice waveforms are displayed.

Generally the CCPLL is able to separate the voice waveforms reasonably well in this example. However, close inspection of the various waveforms reveals certain features that are captured either by the wrong PLL or by both PLLs simultaneously. An example of the latter is the distinct pulse train occurring in the dominant waveform (Figure 2(a)) at about the middle of the three second segment (between approximately 1.4 and 1.5 seconds). The

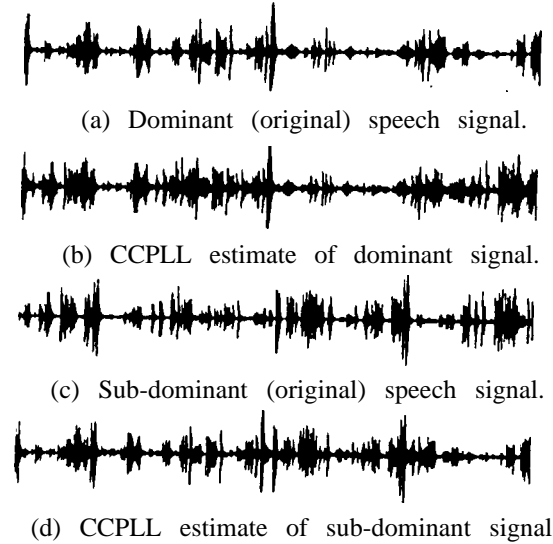


Figure 2: Performance of CCPLL estimator on FM voice signals, each with frequency deviation of 12kHz.

dominant CCPLL estimate (Figure 2(b)) captures this feature but unfortunately so does the sub-dominant (Figure 2(d)). Vice versa at the end of the segment (between approximately 2.8 and 2.9 seconds) the amplitude burst in the sub-dominant waveform (Figure 2(c)) is captured only by the dominant CCPLL estimate.

This phenomenon of “signal switching” is created by a number of factors including instantaneous frequency crossing which causes the individual PLLs to lock onto and track the wrong signals. This problem is less severe as the occurrence of instantaneous frequency crossings is reduced. This situation can be simulated using the same synthesized voice waveforms considered above in Figure 2 but using different FM modulation parameters. For example, if we increase the FM deviation frequency of the sub-dominant from 12 kHz to 24 kHz (with all other modulation parameters the same) and correspondingly open up the PLL bandwidths (again following the CCPLL design rules provided in [6]), we obtain much better voice separation as seen in Figure 3.

Now the objectionable signal switching has been significantly reduced. Of course in practice the presence of instantaneous frequency crossings in the input co-channel data cannot be controlled. Thus the utility of the CCPLL will generally be limited unless some means of compensation can be developed to mitigate the deleterious effects of instantaneous frequency crossings. Possible methods include the inclusion of Kalman tracking techniques that will track previous PLL phase estimates and use these estimates to prevent signal phase switching. This is an area of current research.

The PTC [3] also comprises two PLLs but, both are

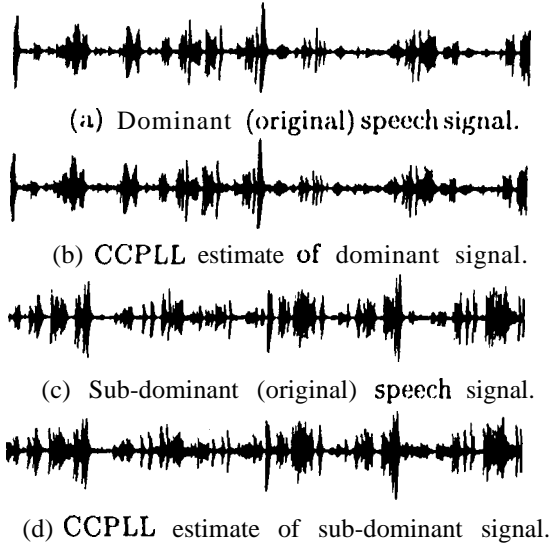


Figure 3: Performance of CCPLL estimator on FM voice signals, with frequency deviations of 12kHz and 24kHz.

used to capture and lock onto the dominant signal, i.e., the first PLL captures the dominant while the second further smoothens the dominant phase estimate as well as inverts its polarity (sign) so that it can be subtracted from the IF input thereby recovering the sub-dominant.

The PTC provides an interesting alternative to the CCPLL in that it reduces the complicated nonlinear dynamics inherent in the CCPLL. However, a key limitation is that amplitude adjustment is required to obtain optimal dominant signal cancellation at the IF. This is typically performed manually which is a clear limitation in operational scenarios — especially in an amplitude-fading environment.

An example showing PTC performance, when the amplitudes of the co-channel signals are presumed known, is presented in Figure 4 for a very short (50 msec) simulated segment. In this example two synthesized voice signals (approximately 3 kHz bandwidth) are FM-modulated and linearly combined using the following parameters from Equation (1):  $A_1 = 1$ ,  $A_2 = 0.5$ ,  $k_1 = 2\pi(70\text{kHz})$ ,  $k_2 = 2\pi(14\text{kHz})$ ,  $\omega_1 = 2\pi(455\text{kHz})$ , and  $\omega_2 = 2\pi(450\text{kHz})$ . Thus, the sub-dominant IF bandwidth is considerably smaller than the dominant IF bandwidth (approximately 25% of the dominant bandwidth), and the IF carrier frequencies are chosen differently. So although there is still significant spectral overlap between the two signals, this example is not as stressing as the previous examples (Figures 2 and 3).

Both the original and PTC-reconstructed estimates (demodulated by the PLLs) for the dominant and sub-dominant synthesized voice waveforms are displayed. As can be seen there is virtually perfect agreement between

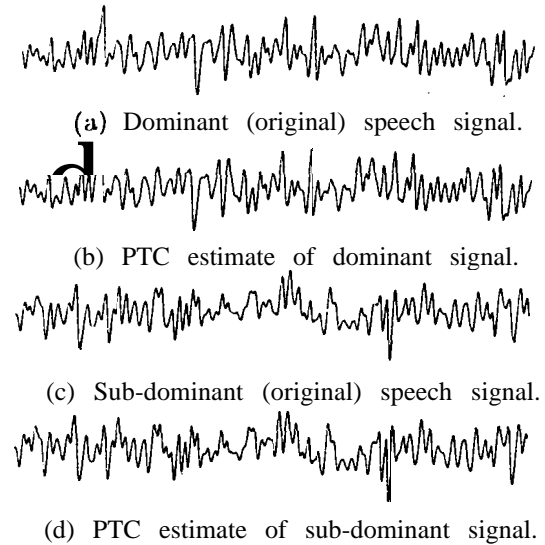


Figure 4: PTC performance on FM voice signals.

the originals and their estimates. Additional simulation experiments with comparable co-channel signal IF bandwidths reveal that the PTC remains very effective in signal separation under the assumption of constant and known signal amplitudes. The next step in our research is to incorporate some form of dominant amplitude estimation into the PTC structure.

#### MAXIMUM LIKELIHOOD SEPARATION

In the case of no interference ( $A_2 = 0$  in Equation (1)), Cahn [1] derived an approximation

$$\hat{r}(t) = A_1 \cos(\omega_1 t + \hat{\theta}_1(t))$$

of  $r(t)$  by minimizing  $\int \|\hat{r}(t) - r(t)\|^2 dt$  subject to the constraint that within successive time intervals of duration  $\Delta t$ ,  $\hat{\theta}''(t)$  is a constant and equal to either  $-C$  or  $C$ . That is, the second derivative of the phase is quantized and used to derive  $\hat{\theta}(t)$ , which in turn is used to determine  $\hat{r}(t)$ . Achieving the closest approximation of  $r(t)$  requires the proper estimation (quantization) of  $\hat{\theta}''(t)$ . Since  $\hat{\theta}(t)$  depends not only on  $\hat{\theta}''(t)$  but also on  $\hat{\theta}''(s)$ ,  $s < t$ , the estimator needs to contain memory. For example, each state of a 16-state trellis corresponds to a quantized value ( $\pm C$ ) of  $\theta''(t)$ ,  $\theta''(t - \Delta t)$ ,  $\theta''(t - 2\Delta t)$ , and  $\theta''(t - 3\Delta t)$ , where  $\Delta t$  is the sampling period.

The Viterbi algorithm chooses one of two values for  $\hat{\theta}''(t)$  in precisely the same way that a maximum likelihood sequence estimator chooses between demodulated bits 0 or 1. Thus, this is a maximum likelihood estimate of  $r(t)$ , provided the constraint  $\theta''(t) = \pm C$  is an accurate one.

We extend Cahn's idea to the case of  $A_2 \neq 0$  by jointly estimating  $\theta_1(t)$  and  $\theta_2(t)$ . That is,  $r(t)$  is estimated by

$$\hat{r}(t) = A_1 \cos(\omega_1 t + \hat{\theta}_1(t)) + A_2 \cos(\omega_2 t + \hat{\theta}_2(t)), \quad (2)$$

and maximum likelihood estimation is performed as before. The new trellis size for joint estimation is the square of Cahn's trellis size. However, the increase in computing power since Cahn's 1974 paper has allowed us to simulate three bits of memory for each signal (64 states) with excellent results.

The algorithm is implemented in a discrete environment. We define the discrete versions of the functions in the usual way, i.e.,  $r[n] = r(n\Delta t)$ ,  $\theta[n] = \theta(n\Delta t)$ , etc. To determine  $\hat{r}[n]$ , the following update equations are used, for  $i = 1, 2$ :

$$\begin{aligned} \hat{\theta}'_i[n] &= \hat{\theta}'_i[n-1] + \hat{\theta}''_i[n]\Delta t \\ \hat{\theta}_i[n] &= \hat{\theta}_i[n-1] + \hat{\theta}'_i[n]\Delta t + \hat{\theta}''_i[n](\Delta t)^2/2, \end{aligned}$$

and  $\hat{r}[n]$  is determined from Equation (2).

Because of the quite general modeling of the received waveform, this technique is potentially applicable to a wide class of CCI problems, including both analog signals (FM, PM) and digital signals (FSK, MSK, PSK, QAM, etc.)—indeed, any signal which can be written in the form of Equation (1). The Viterbi algorithm merely attempts to approximate the received signal by the sum of two waveforms; it requires no knowledge of the modulation or timing of the waveforms. Incorporation of this knowledge allows improved performance for specific applications such as BPSK/BPSK interference, which will be discussed in the following section.

Figure 5 indicates the performance of the joint Viterbi algorithm on co-channel FM voice signals. The modulating signals are synthesized voice, and the parameters chosen are identical to those used in Figure 2. That is, the subdominant signal power is 6dB below the dominant signal power, the frequency deviation is 12kHz for each signal, and there is no carrier offset for either signal, i.e., we assume the carrier has already been removed. The received signal was again sampled at 131kHz. As can be seen, nearly all features of each signal are recovered and separated into the dominant and subdominant signals, with virtually no signal switching occurring. This is especially significant in view of the fact that the modulating signals are statistically identical, and equal frequency deviations are used. When real voice signals are used, both signals are easily intelligible, with the dominant signal suffering almost no degradation in sound quality. The quality of the subdominant signal is somewhat degraded.

Figure 6 indicates the performance of the joint Viterbi algorithm on BFSK co-channel interfering signals. The modulating signals are determined from independent,

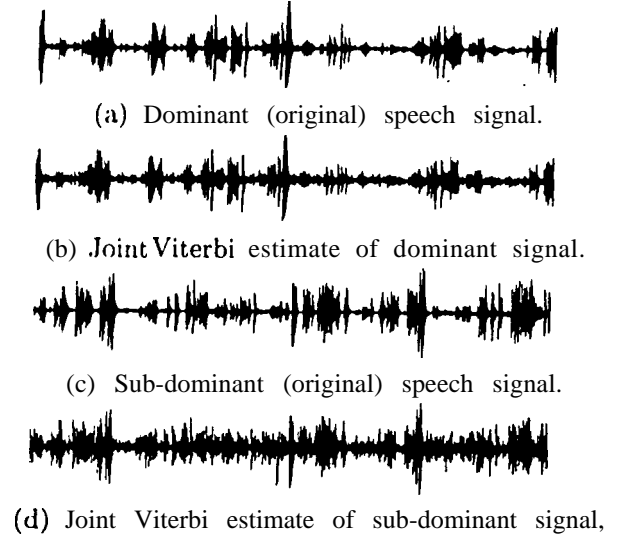


Figure 5: Performance of joint Viterbi estimator on CCI FM voice signals.

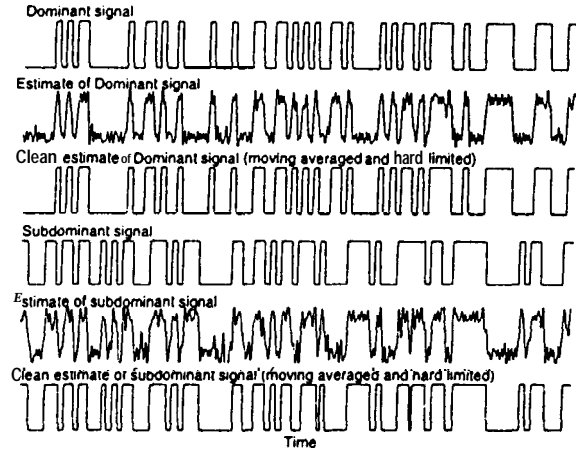


Figure 6: Joint Viterbi estimation of CCI BFSK signals.

uniformly distributed bit streams, each at a baud rate of 10,000 bits per second. A rectangular pulse shape is used, and the interfering signals were offset by 1/4 bit. The parameters used in Equation (1) are  $A_1 = 1$ ,  $A_2 = 0.5$ ,  $k_1 = k_2 = 2\pi(5\text{kHz})$ , and  $w_1 = w_2 = 0$ . The received signal was sampled at 40kHz, i.e., there were 4 samples per bit. As can be seen, the raw output of the Viterbi algorithm recovers much of the information of the original signals: when a moving average and hard limiter are applied the original and estimated signals match almost perfectly.

In practice, the receiver does not have a priori knowledge of  $A_1$  and  $A_2$ , and these quantities must also be estimated at the receiver. We used the LMS algorithm to adaptively estimate  $A_1$  and  $A_2$ . To improve perfor-

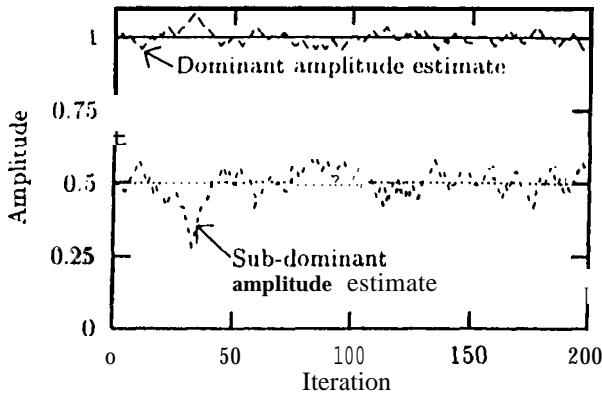


Figure 7: Amplitude estimates for two statistically identical FM voice waveforms. The true amplitudes were constant, as shown.

mance, the estimates were updated in per-survivor processing (PSP) fashion, i.e., separate estimates were stored at each state of the trellis, instead of one estimate at each time step [4]. We found that the estimates accurately track the true values, as shown in Figure 7. (In this case, the estimate itself is quite good but can be improved further by applying a moving average to the estimate.) As a result, there was virtually no difference in the quality of the  $\hat{r}(t)$  estimate when working with known amplitudes or estimated amplitudes. This method also tracks amplitudes which vary slowly in time.

It is clear how this joint estimator may be extended to more than two interfering signals with the addition of more trellis states. Since the trellis size grows exponentially in the number of interfering signals, there is a practical limit to the model, however.

#### MAXIMUM LIKELIHOOD DEMODULATION OF BPSK SIGNALS IN THE PRESENCE OF MULTIPATH AND CO-CHANNEL INTERFERENCE

Here we briefly discuss the application of ML-based methods to the demodulation of BPSK signals in the presence of multipath and co-channel BPSK interference. In particular, we consider further the joint trellis algorithm originally presented in [5] as it applies to co-channel BPSK demodulation and channel estimation in the presence of static and fading multipath. This algorithm represents a significant departure from the joint Viterbi algorithm presented above in that it estimates the data symbols directly as opposed to the (continuous-time) phase waveforms. The underlying system assumed here is modeled as a band-space d, or  $T$ -spaced, baseband digital communication system, i.e., the BPSK data symbols for both the desired signal and interferer are transmitted in a  $T$ -

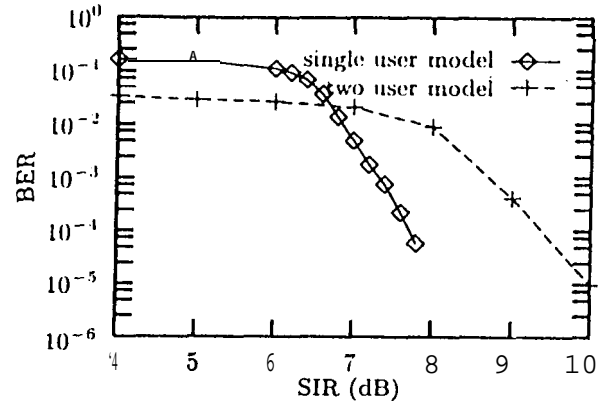


Figure 9: Static channel bit error rate results for both a joint and single trellis demodulation algorithm.

spaced data sequence. The corresponding envelope of the received signal is formed by convolving both desired and interference BPSK waveforms with generally different  $T$ -spaced channel impulse responses (CIRs) and then linearly combining the convolved waveforms. It is assumed (at least initially in our studies) that no additive noise is present and that the received desired signal and interferer are synchronous and that perfect symbol timing is available. Performance metrics are the bit error rate (BER) of the desired signal and the received signal-to-interference power ratio (SIR).

Two simulation examples are considered here. The first corresponds to a static multipath environment wherein both the desired and interference multipath channels are modeled by a  $T$ -spaced CIR with two equal non-zero taps. The tap value for the desired multipath channel is unity whereas the corresponding value for the interference channel is varied to achieve different values of SIR. Plots of BER versus SIR are presented in Figure 8 corresponding to both a joint trellis algorithm (with 2 states allocated each to the desired signal and interferer for a total of  $2 \times 2 = 4$  states) and a single trellis algorithm (modeling only the desired signal with a total of 2 states). Both algorithms are initialized with a single (2 state) trellis which is trained using a known, desired signal sequence. The purpose of this training interval is to obtain an estimate of the desired multipath taps. Then, in the case of the joint trellis algorithm, the trellis is expanded to 4 states after the desired signal training sequence in order to estimate the interference multipath channel (in the blind) and in the process demodulate the desired BPSK signal.

As is seen from Figure 8, the joint trellis algorithm provides a BER  $< 3\%$  at all SIRs between 4 and 10 dB. However, once the SIR exceeds 7 dB, the single trellis outperforms the joint trellis and so it is better to discard the states allocated to the interferer once its power

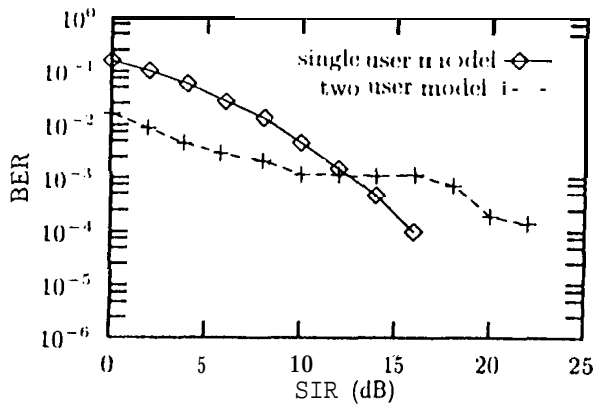


Figure 9: Fading channel bit error rate results for both a joint and single trellis demodulation algorithm,

falls below a certain (threshold) level. This behavior is a consequence of the initialization process described above, i.e., once the interference power becomes too small the resulting estimate of the interference multipath channel (derived blindly by the joint trellis) is too noisy to yield good demodulation of the desired signal and hence the single trellis algorithm provides the best performance.

Similar results are obtained in a simulated slow Rayleigh fading multipath environment wherein both the desired signal and interference channels are modeled by independent, three tap (T-spaced) channels. Each tap is fading independently with the same average power. The average tap power is unity for the desired signal channel and is varied for the interference channel to achieve different values of average SIR. Plots of BER versus SIR are presented in Figure 9 corresponding to both a joint trellis algorithm (with 4 states allocated each to the desired signal and interferer for a total of  $4 \times 4 = 16$  states) and a single trellis algorithm (modeling only the desired signal with a total of 4 states). Both algorithms are initialized as described above (but using 4 states per co-channel signal instead of 2 states). Again it is seen that the single trellis algorithm outperforms the joint trellis when the SIR exceeds a certain level (12 dB in this case).

#### CONCLUSIONS

The CCPLL is extremely effective at separating an FM voice signal from an unmodulated carrier signal, but it suffers from occasional "signal switching" if the subdominant signal has modulation parameters very similar to those of the dominant, signal. The PTC also separates FM voice signals very well for the cases tested, but in its present state, it is of limited practical utility because a priori knowledge or a manual estimate of the dominant signal amplitude is required. Two versions of a joint Viterbi algorithm were presented. The first is based on Cahn's approach [1] and can be applied to a wide variety

of analog and digital signals. Results with this algorithm using a 64-state trellis revealed very good demodulation of digital BFSK signals and furthermore yield co-channel FM voice separation without the "signal switching" associated with the CCPLL. The second type of joint Viterbi algorithm considered [5] yields direct data symbol estimates in multipath environment, s. The application of this algorithm to both static and fading multipath channels reveals that once the interference power falls below a certain threshold level, it is better to discard the joint trellis architecture and just model the desired signal states.

#### REFERENCES

- [1] C. R. Cahn, "Phase tracking and demodulation with delay," *IEEE Trans. Inform. Theory*, vol. IT-20, no. 1, pp. 50-58, Jan. 1974.
- [2] F. Cassara, H. Schachter, "Suppression of interchannel interference in FM receivers," Polytechnic Report, POLY EE79-056, Polytechnic Institute of New York, Farmingdale, NY, July 1979.
- [3] G. Myers, "Multiple reuse of an FM band," US Patent No. 489958, August 22, 1989.
- [4] R. Raheli, A. Polydoros, and C.-K. Tzou, "Per-survivor processing: a general approach to MLSE in uncertain environments," *IEEE Trans. Comm.*, vol. 43, no. 2/3/4, pp. 354-364, Feb./Mar./Apr. 1995.
- [5] A. Polydoros, G. Paparisto, "Per-survivor processing for joint data/channel estimation in multipath fading and co-channel interference channels," Proceedings of MILCOM'95 (Classified), La Jolla, CA, Nov. 5-8, 1995.
- [6] S. Say, "Vector-locked loop interference canceler," Ph.D. dissertation, Polytechnic Institute of New York, June 1985.
- [7] J. Zimmerman, "applications of frequency modulation interference cancelers to multi-access communication systems," Ph.D. Dissertation, California Institute of Technology, Pasadena, CA, 1990.